A Fresh View of Global Atmosphere and Ionosphere from the Combined GNSS-RO (Radio Occultation) Constellations

Dong L. Wu

NASA Goddard Space Flight Center, Code 613

Acknowledgments:

- Contributions from Daniel Emmons, Nimalan Swarnalingam, Manisha Ganeshan, Jie Gong, Tyler Summers
- Fundings from NASA's Programs: Commercial Smallsat Data Acquisition (CSDA), GNSS Science Team, Living With Star (LWS), and Sun-Climate Research

Global Navigation Satellite Systems (GNSS) Radio Occultation (RO)

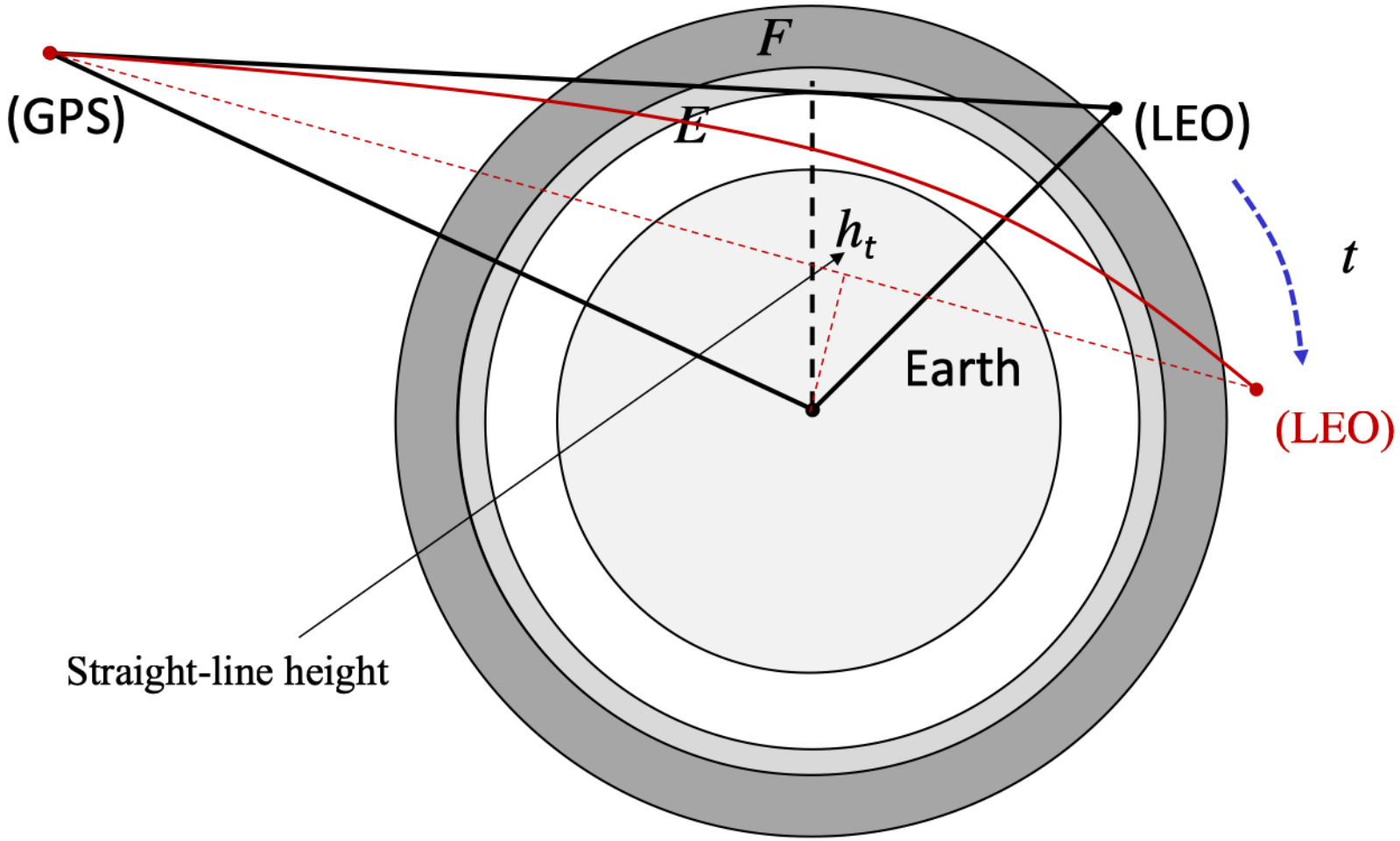

RO Amplitude

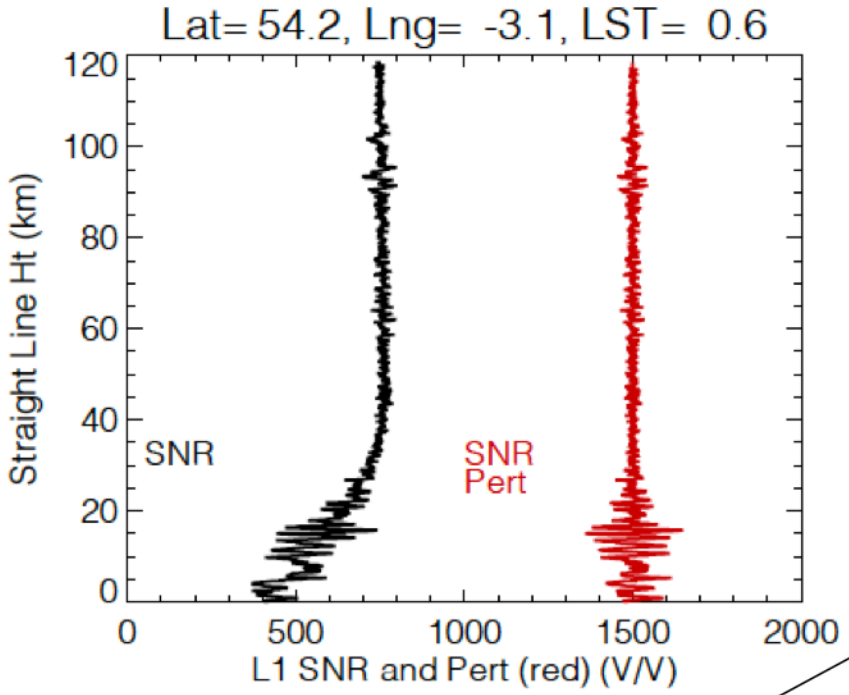

RO Excess Phase

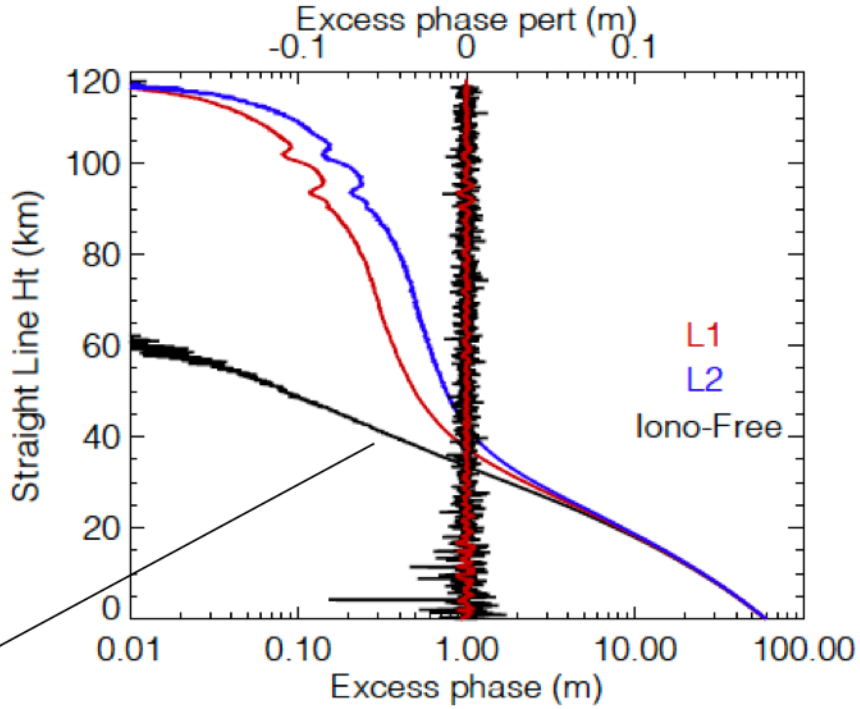

$$N = (n-1)\times 10^6 = \underbrace{76.6\frac{P}{T} + 3.73\times 10^5\frac{P_w}{T^2}}_{\text{Operation}} \underbrace{- 4.03\times 10^7\frac{n_e}{f^2} + o(IWP, f^3, f^4)}_{\text{Research}}$$

Wu (Remote Sensing, 2020)

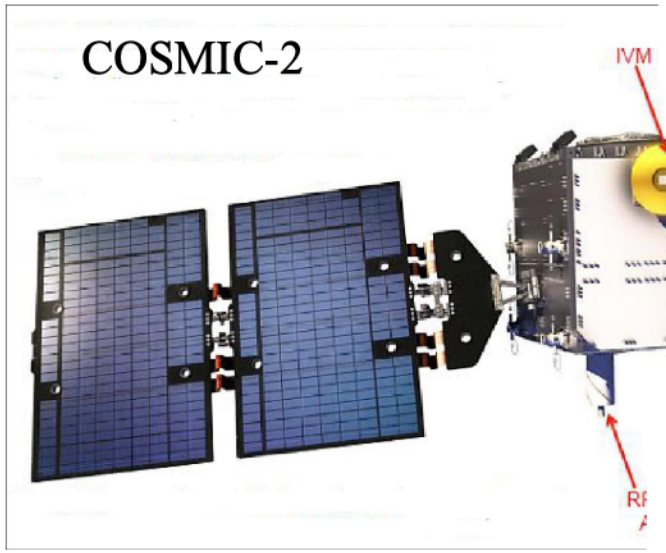

POD antenna

RO antenna

GPS

1 Hz

1 Hz

POD hTEC

50/100 Hz

GPS

GPS

POD antennas (2x)

- Wide FOV
- Low gain
- Low sampling rate
- Absolute hTEC

RO antennas (2x)

- Narrow FOV
- High gain
- High sampling rate
- Relative hTEC

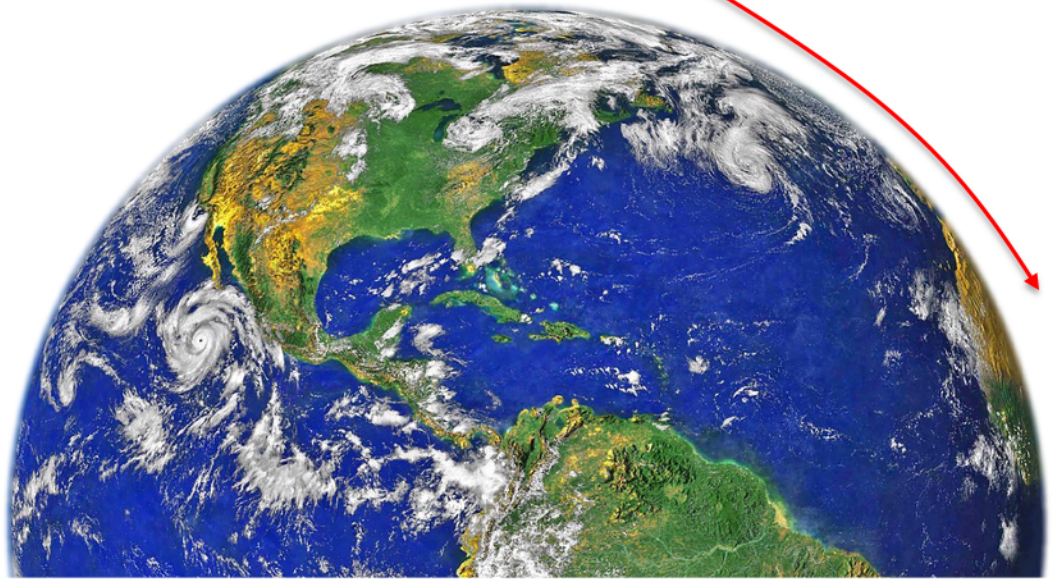

GPS

POD antenna

1 Hz

1 Hz

POD hTEC
(ionosphere)

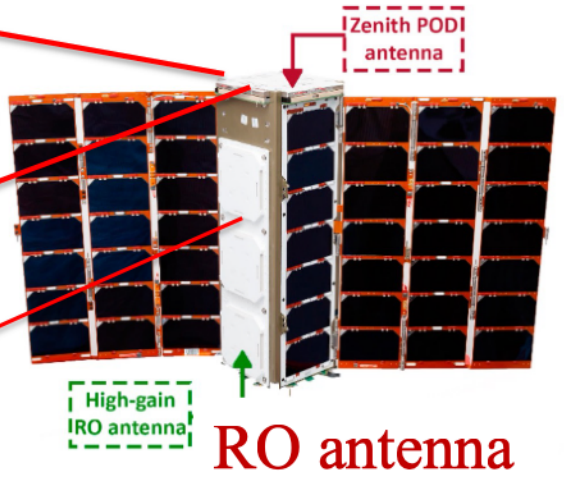

RO antenna

GPS

Atmosphere

50 Hz

GPS

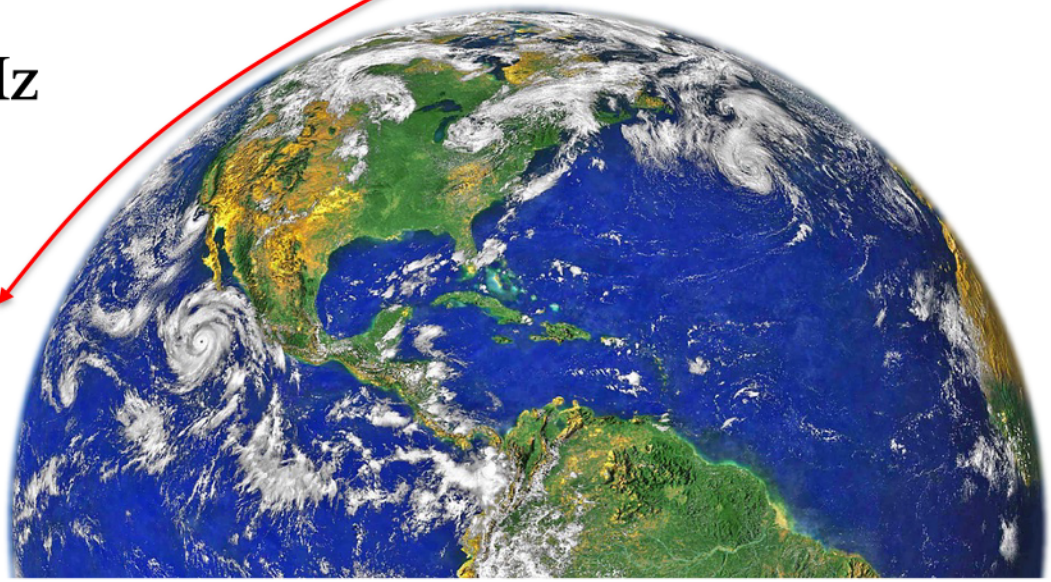

POD antennas (2x)

- Wide FOV
- Low gain
- Low sampling rate
- Absolute hTEC

RO antennas (2x)

- Narrow FOV
- High gain
- High sampling rate
- Relative hTEC

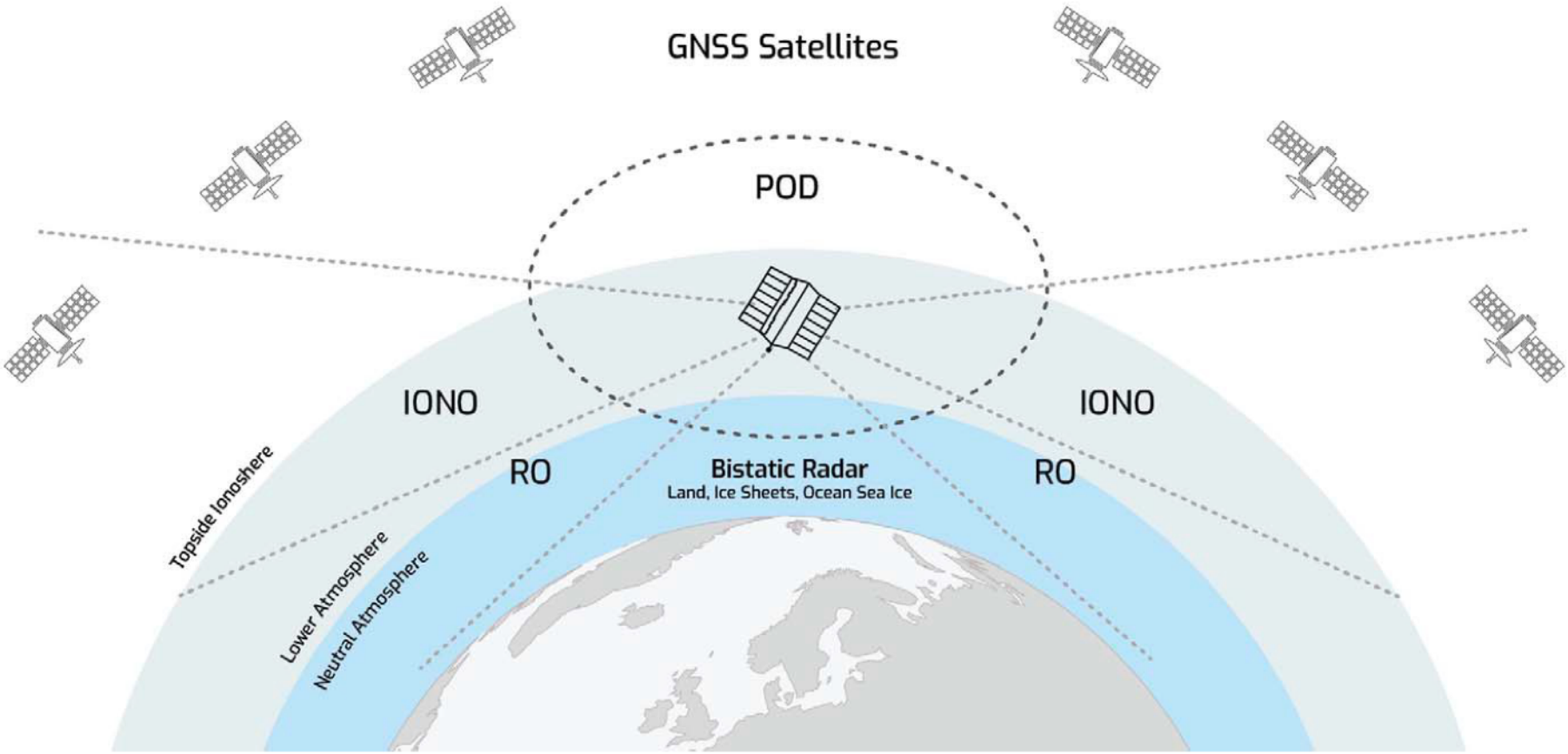

Angling et al. (2021)

Spire Daily GNSS-RO Statistics (L1B: atmPhs)

By flight model (FM)

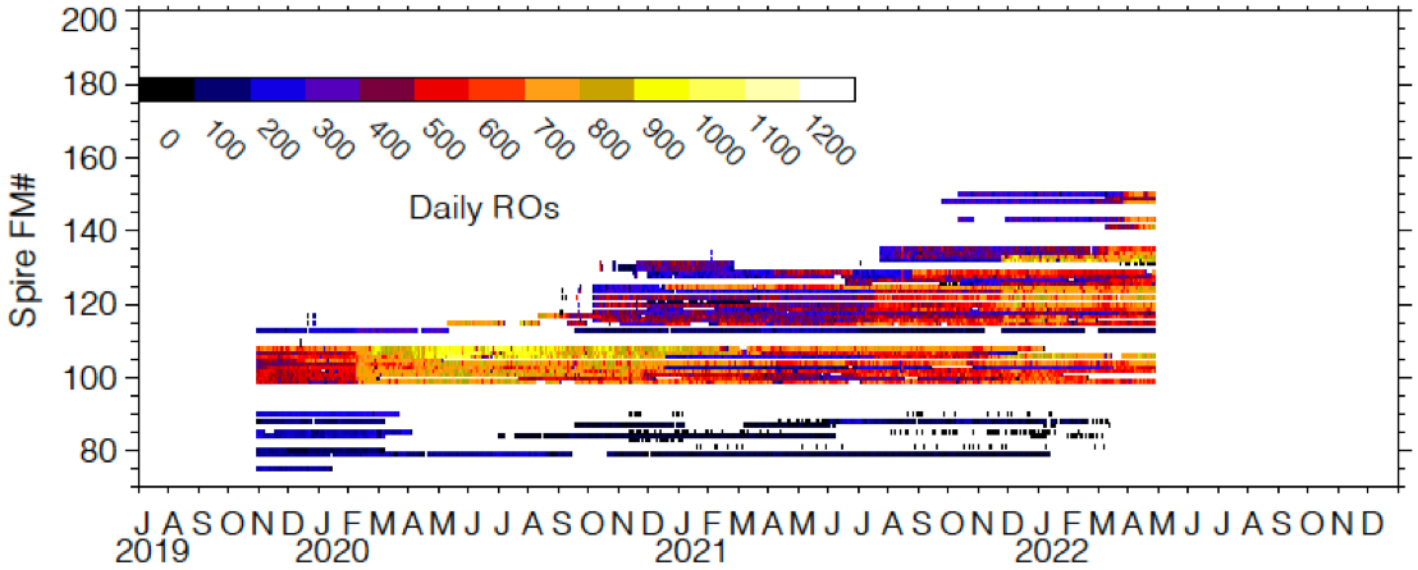

Total daily number

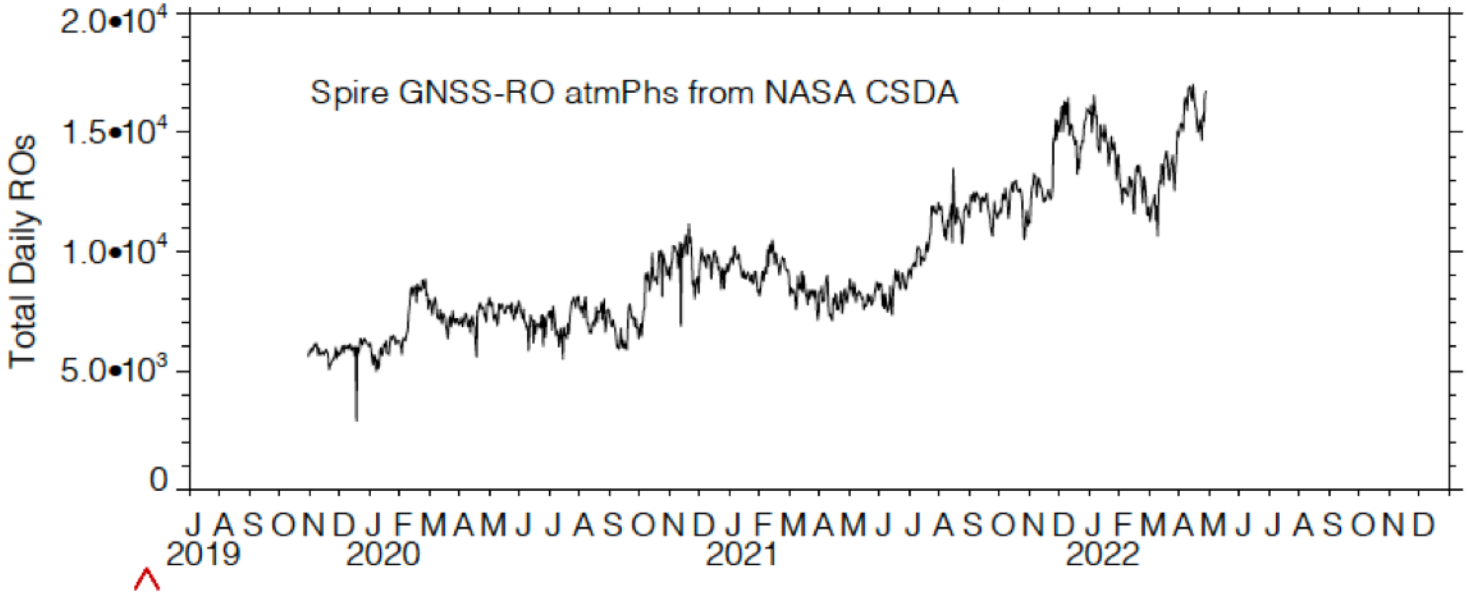

Daily RO Observations Since CHAMP (NASA-DLR)

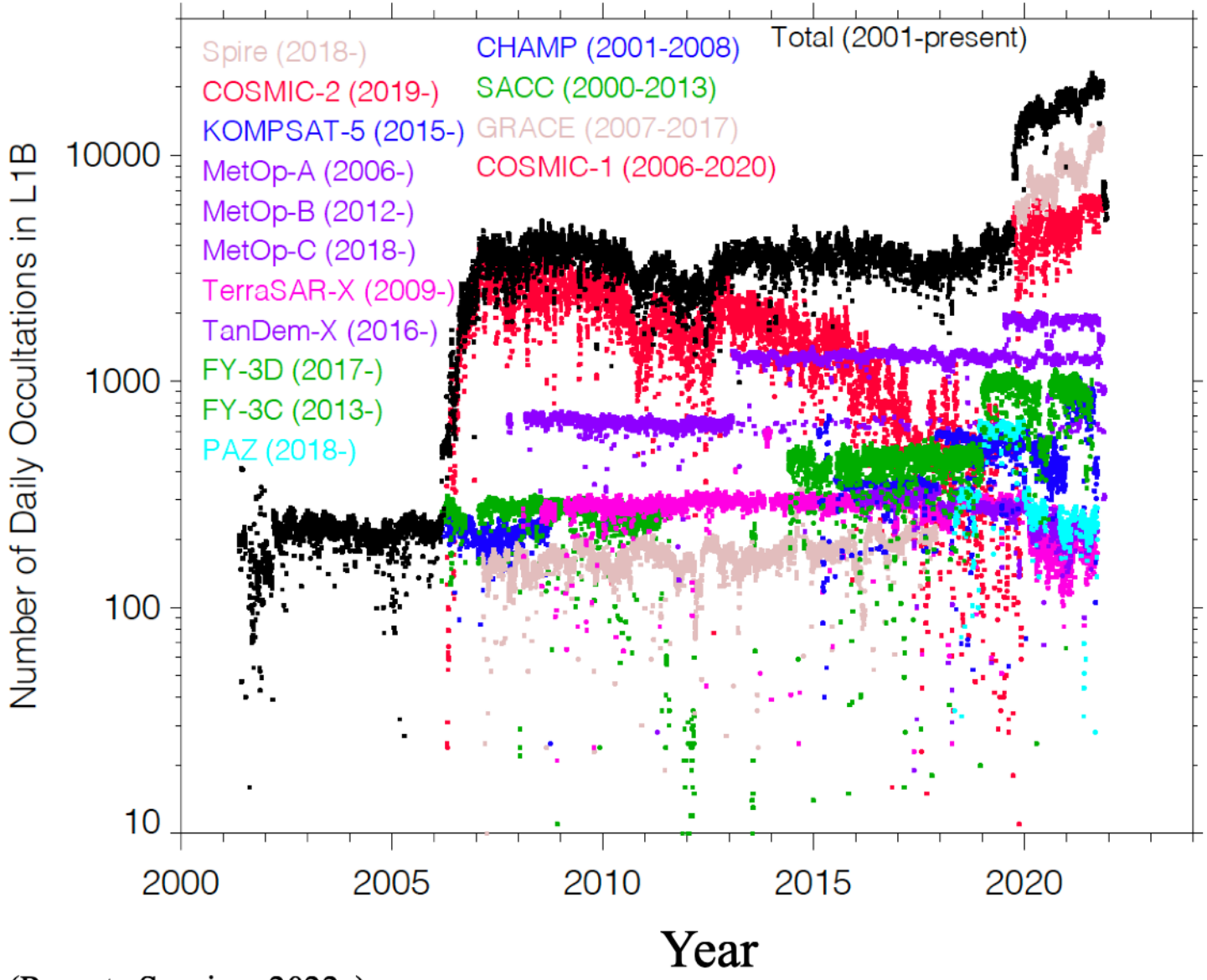

Wu et al. (Remote Sensing, 2022a)

Local Time Sampling

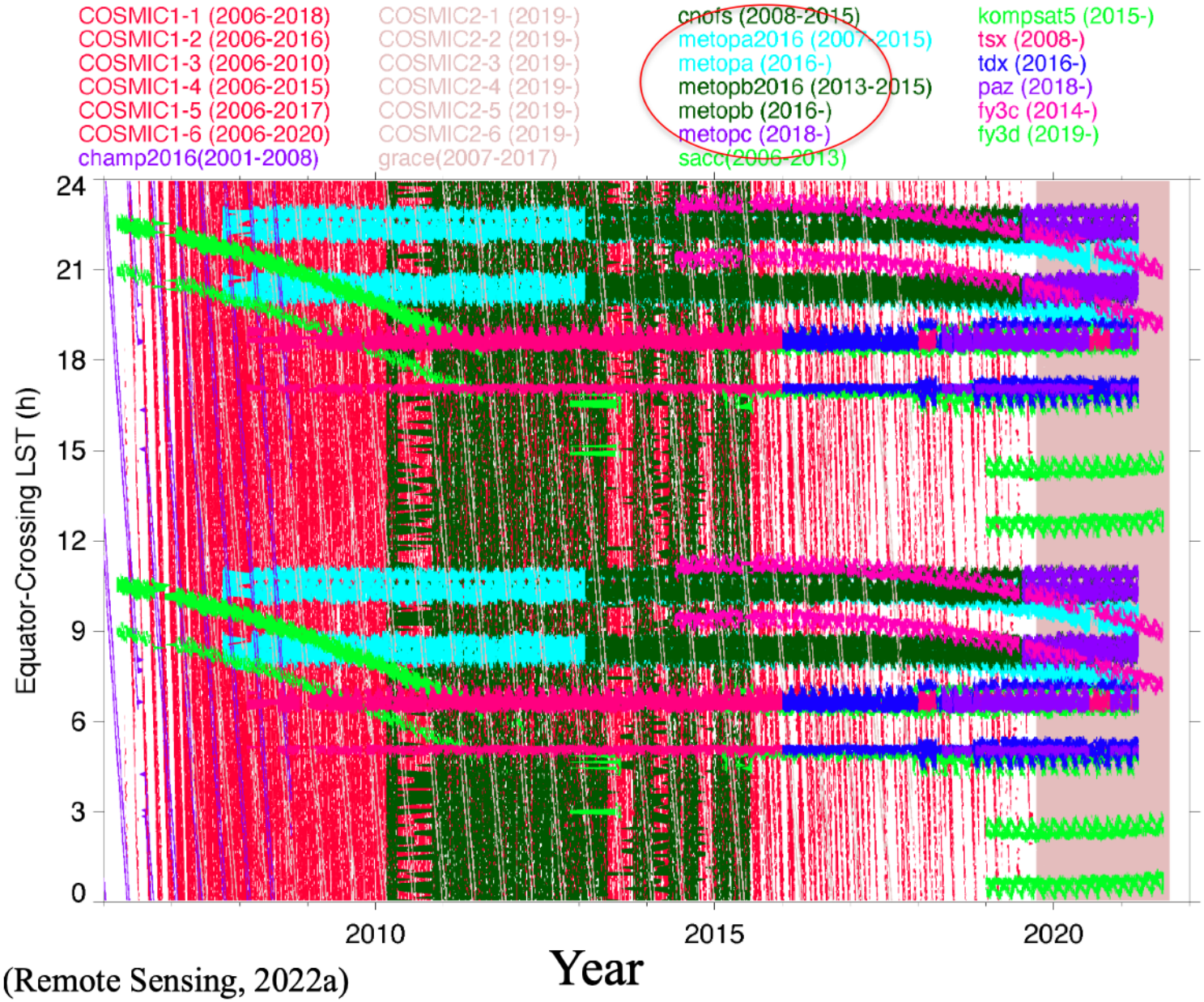

Wu et al. (Remote Sensing, 2022a)

Daily Sampling Maps from GNSS RO

COSMIC-1
(2006-2020)

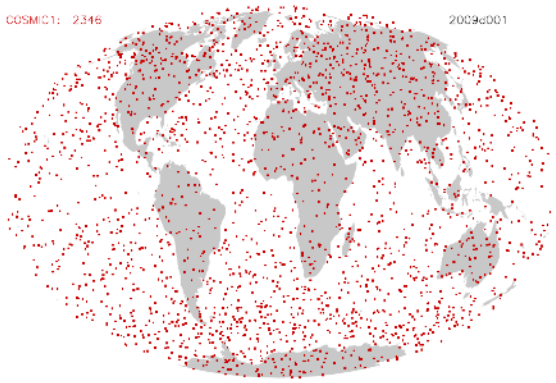

COSMIC-2
(2020-)

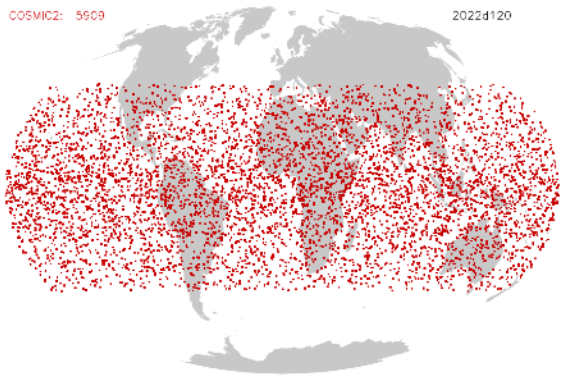

Spire
(2019-)

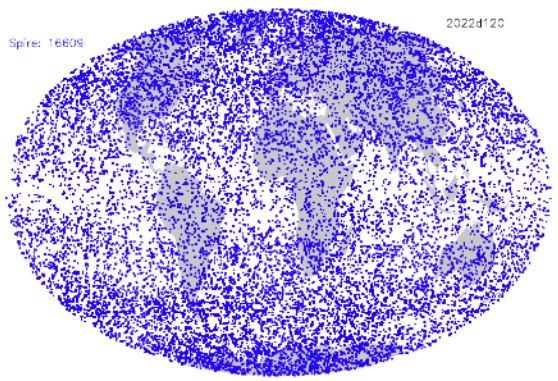

COSMIC-1 + Others (2009d001)

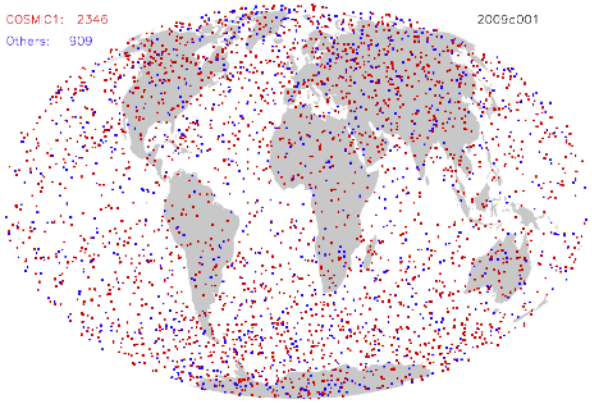

COSMIC-2 + Spire (2022d120)

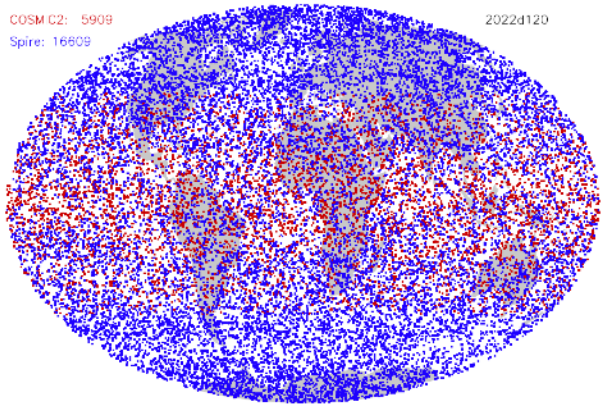

Comparisons of LEO Satellite Dimension and GNSS Tracking

COSMIC-1

D = 100 cm
H = 18 cm

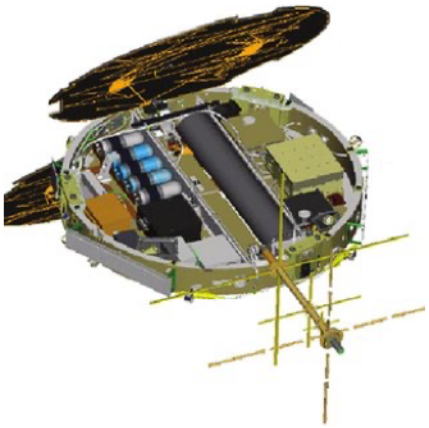

COSMIC-2

(L × W × H)
125 × 100 × 125 cm

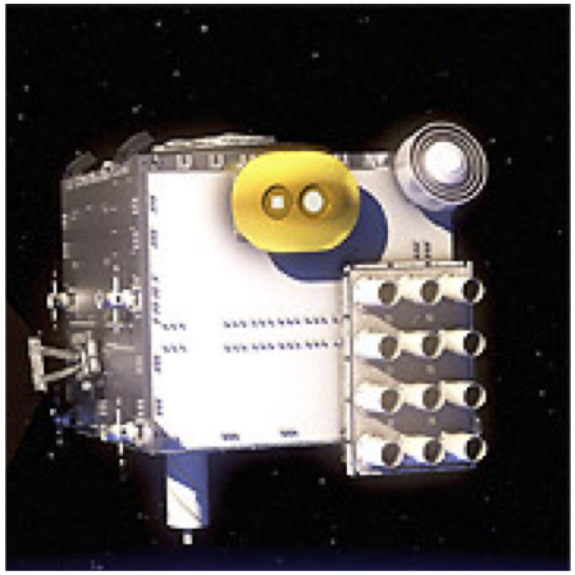

Spire

(L × W × H)
10 × 10 × 30 cm

U.S. NavstarGlobal Positioning System (GPS)
Russia's GLObal NAvigation Satellite System (GLONASS) constellations
European Navigation Satellite System Galileo (Galileo)
Japanese Quasi Zenith Satellite System (QZSS).

GNSS Tracking

COSMIC-1	COSMIC2	Spire
GPS	GPS, GLONASS	GPS, GLONASS, Galileo, QZSS

Sampling Comparisons of GNSS-RO and GNSS-POD

	RO Antennas (Atmos & D/E-Region)		POD Antennas (F-Region)	
	Total L1B	Ne	Total L1B	Ne
COSMIC-1 (Jan 1, 2008)	1,690	1,419	1,832	1,175
COSMIC-2 (Jan 1, 2022)	6,199	6,068	9,366	6,661
Spire (Jan 1, 2022)	15,900	15,756	18,433	5,960

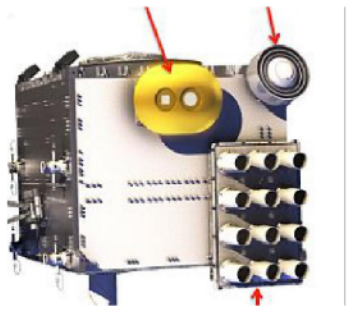

TEC

RO data

TEC

POD data

Atmospheric Sciences

Fraction of SPIRE RO observations reaching PBL (ocean & low, flat land only)

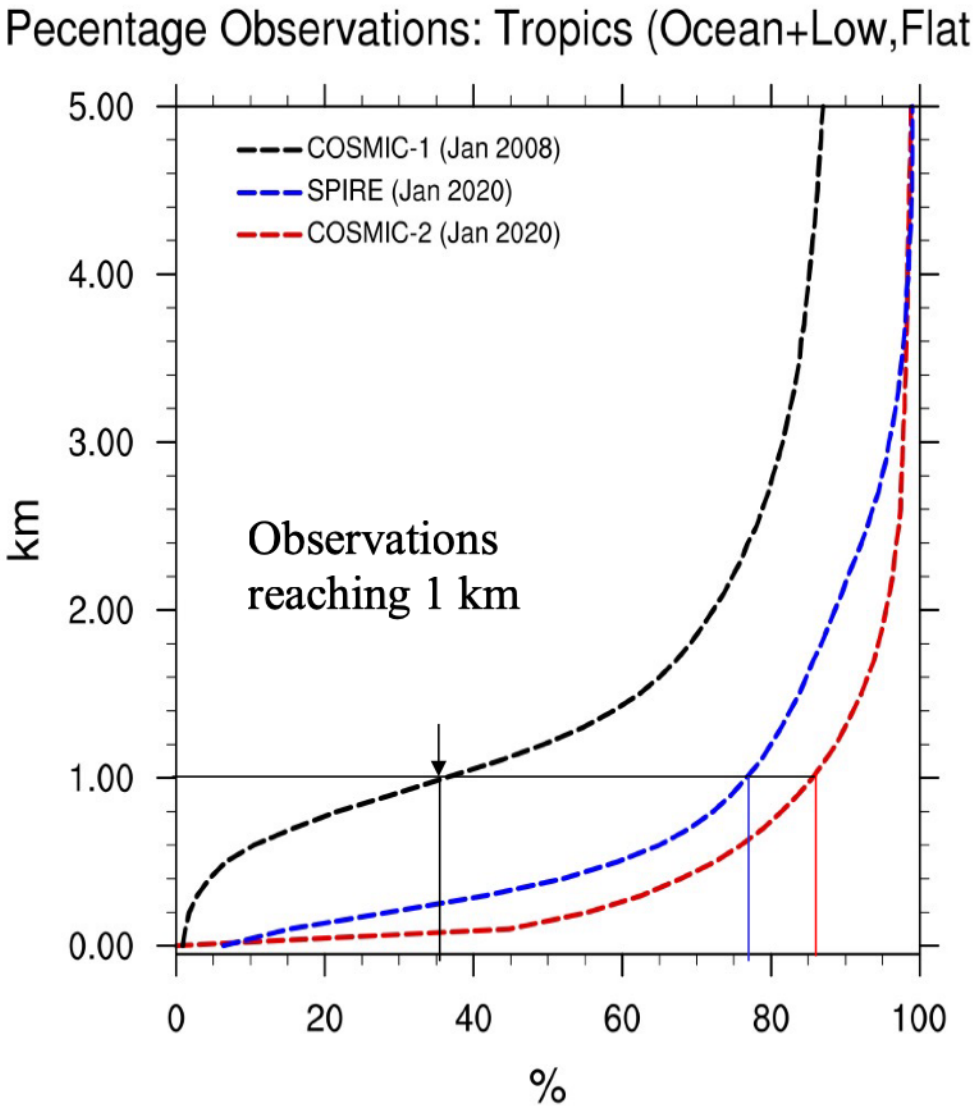

Comparison of **Level-2 atmPrf** Sampling Statistics from Spire, COSMIC-1 and COSMIC-2:

- Spire has generally lower but comparable sampling in PBL;
- Large fraction of SPIRE RO profiles reach 1km level;
- Monthly variability in SPIRE RO penetration (%) evident at 1km level (tropics and NH midlatitude) and 200m level (NH midlatitude and NH polar regions).

(Courtesy of M. Ganeshan)

- Novel method to infer PBL water vapor (q) from GNSS-RO amplitude
- Benefit of global GNSS-RO sampling to study diurnal variations and polar regions

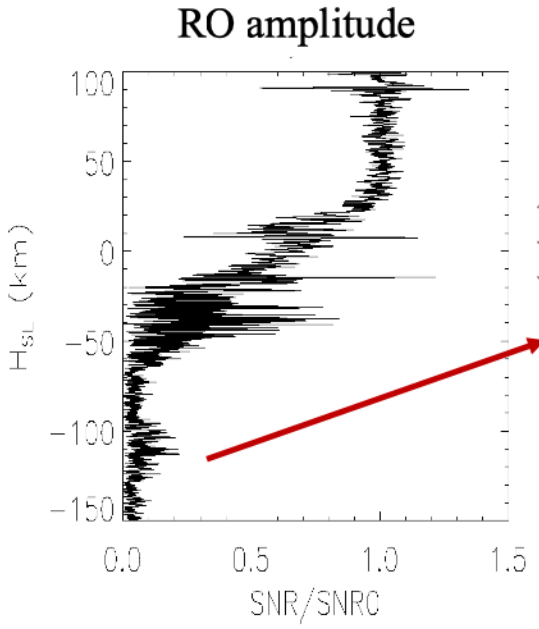

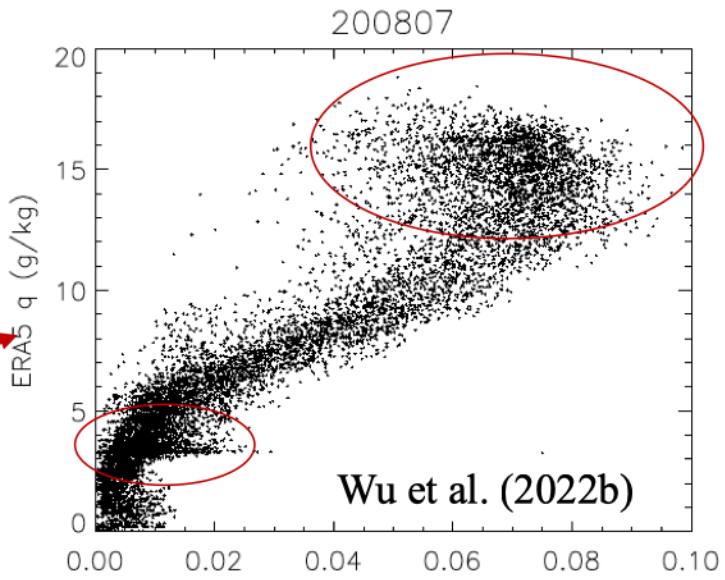

SNR/SNR0 at *ht*=-100 km

Marine Atmos Boundary Layer Water Vapor (q) at 950 hPa

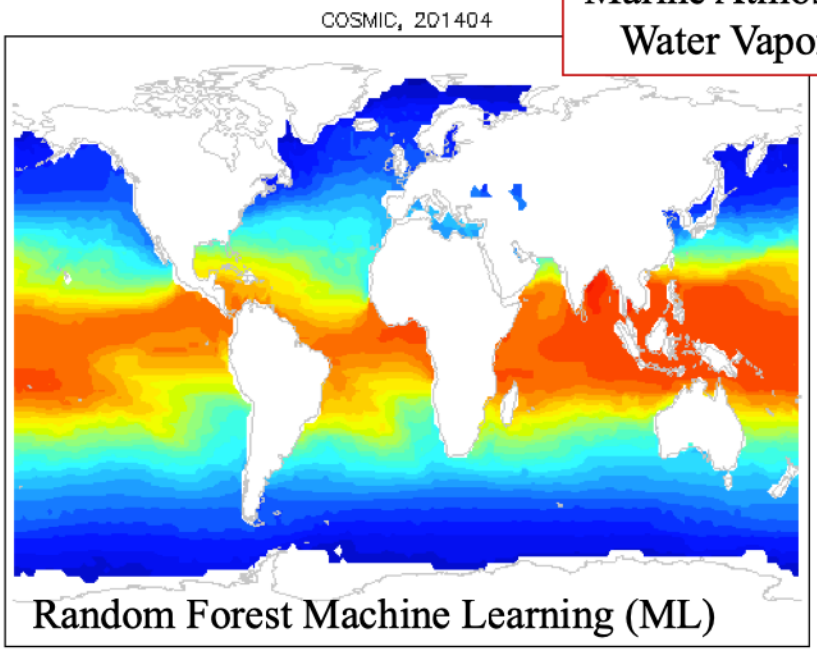

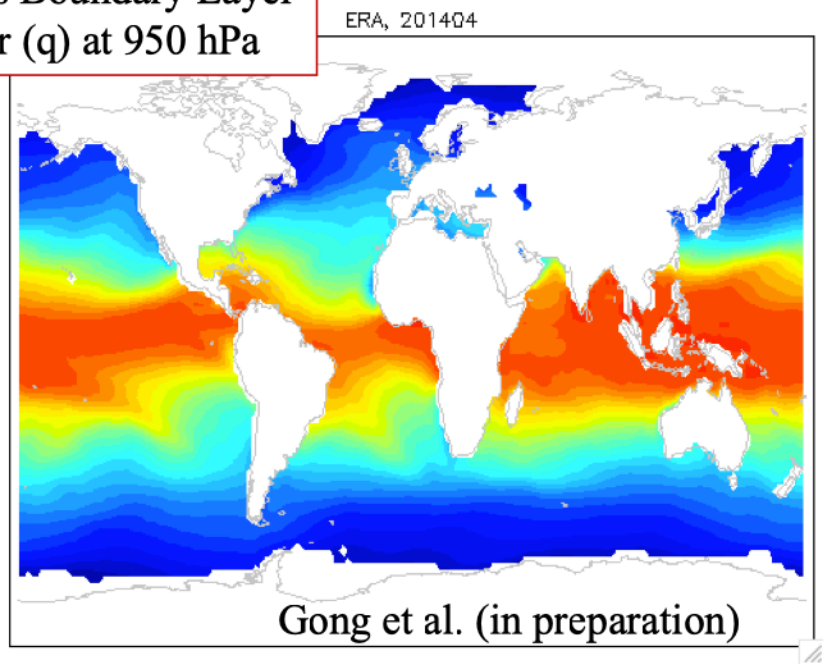

Ionospheric Sciences

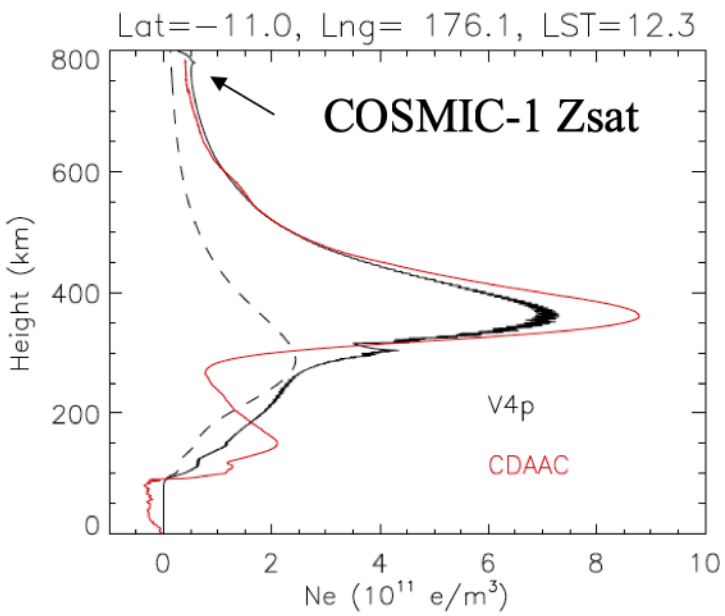

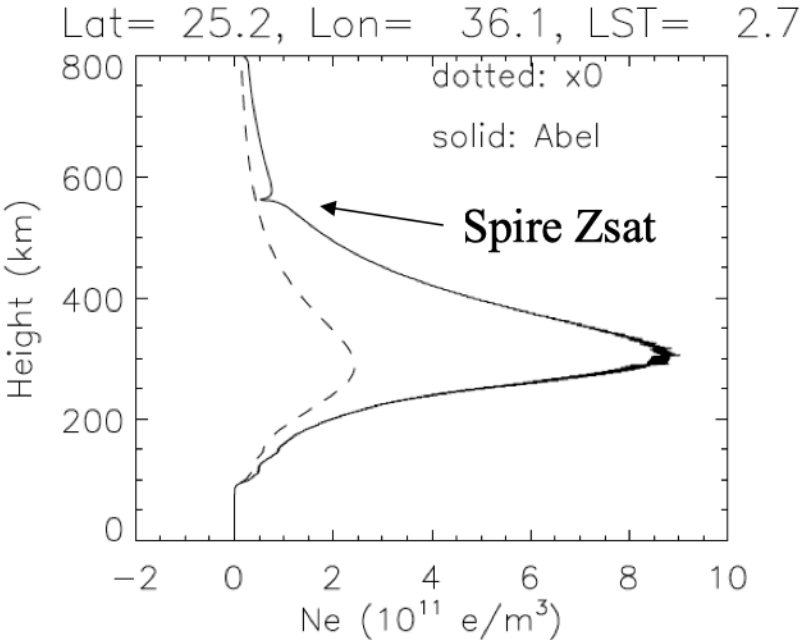

Comparisons with TEC from IGS Network

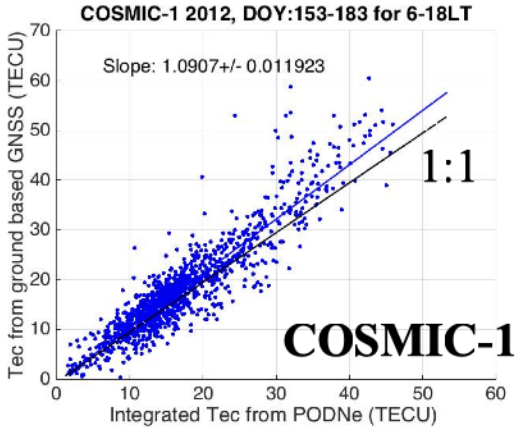

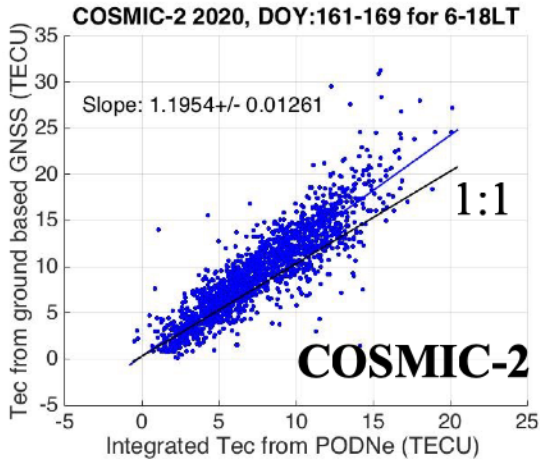

Under evaluation

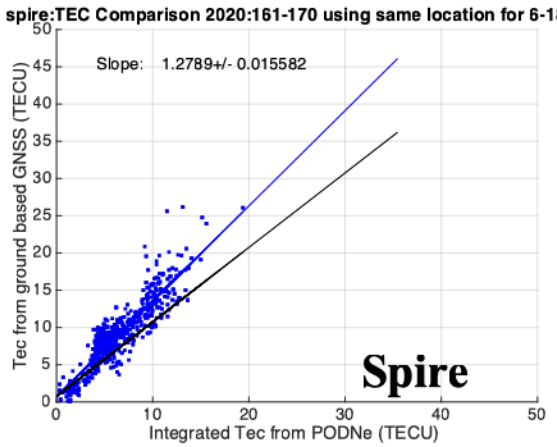

TEC Derived from GNSS-RO Gradient

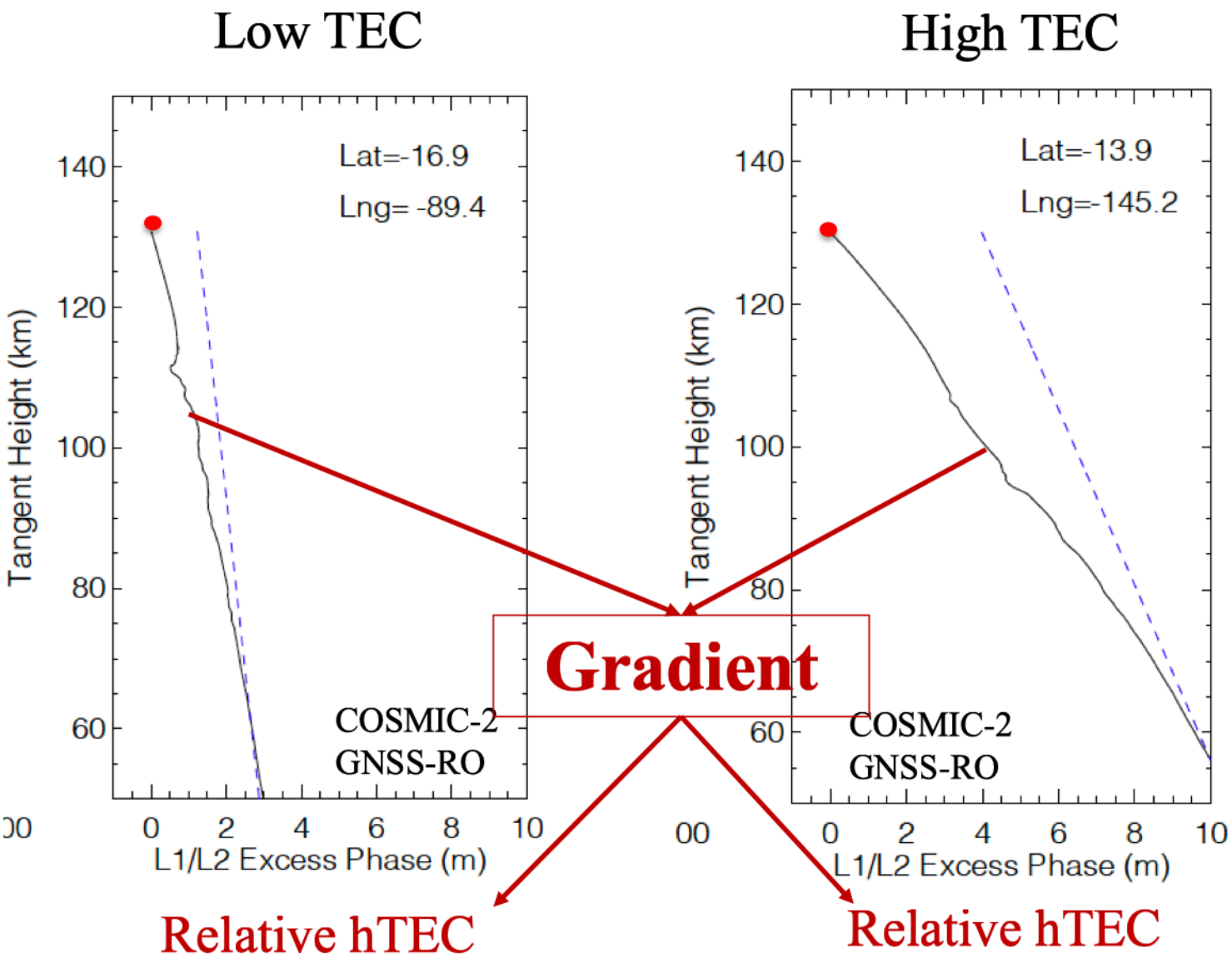

Spire 2-Hourly TEC Maps from Jan 2022

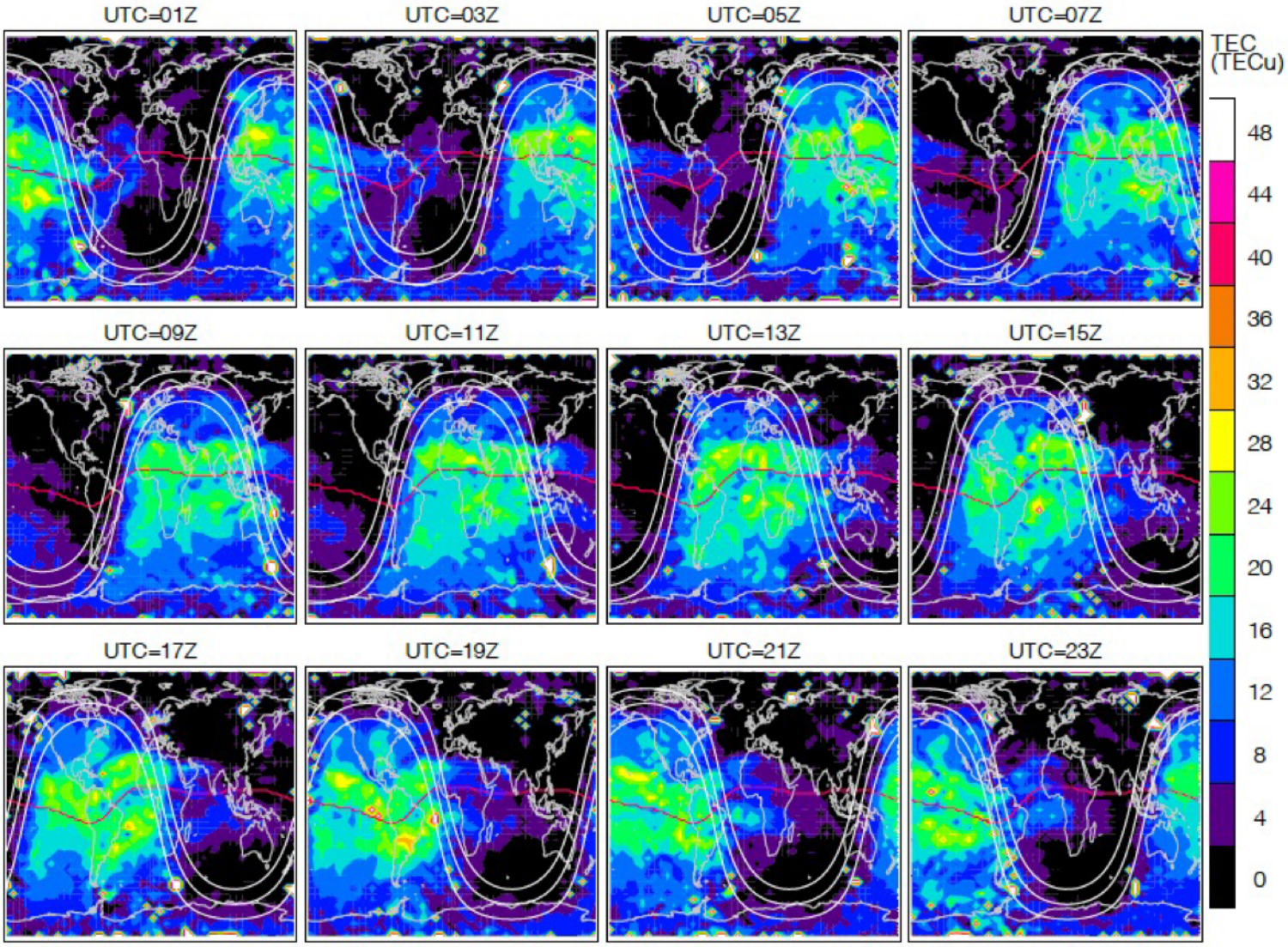

References

- Angling, M. J., et. al. (2021). Sensing the ionosphere with the Spire radio occultation constellation, J. Space Weather Space Clim. 11 56, DOI: 10.1051/swsc/2021040
- Wu, D.L., Ionospheric S4 Scintillations from GNSS Radio Occultation (RO) at Slant Path. Remote Sens. 2020, 2(15), 2373; https://doi.org/10.3390/rs12152373
- Wu, D.L.; Emmons, D.J.; Swarnalingam, N. Global GNSS-RO Electron Density in the Lower Ionosphere. Remote Sens. 2022a, 14, 1577. https://doi.org/10.3390/rs14071577
- Wu, D.L.; Gong, J.; Ganeshan, M. GNSS-RO Deep Refraction Signals from Moist Marine Atmospheric Boundary Layer (MABL). Atmosphere 2022b, 13, 953. https://doi.org/10.3390/atmos13060953
- Wu, D.L., et al. (2023), Optimal Estimation Inversion of F-Region Electron Density from GNSS-POD Measurements: Part I. Algorithm and Data Reduction, in preparation.
- Swarnalingam, N., et al. (2023), Optimal Estimation Inversion of F-Region Electron Density from GNSS-POD Measurements: Part II. Validation of hmF2 and NmF2, in preparation.